THE INFLUENCE OF PREBUCKLING DEFORMATIONS AND STRESSES ON THE BUCKLING OF PERFECT CYLINDERS

by Manuel Stein

Langley Research Center
Langley Station, Hampton, Va.

NATIONAL AERONAUTICS AND SPACE ADMINISTRATION • WASHINGTON, D. C. • FEBRUARY 1964

THE INFLUENCE OF PREBUCKLING DEFORMATIONS AND STRESSES ON THE BUCKLING OF PERFECT CYLINDERS

By Manuel Stein

Langley Research Center
Langley Station, Hampton, Va.

NATIONAL AERONAUTICS AND SPACE ADMINISTRATION

For sale by the Office of Technical Services, Department of Commerce,
Washington, D.C. 20230 -- Price $0.50

THE INFLUENCE OF PREBUCKLING DEFORMATIONS AND STRESSES ON THE BUCKLING OF PERFECT CYLINDERS

By Manuel Stein

SUMMARY

Large-deflection theory is used to compute buckling loads of simply supported initially perfect cylinders under axial compression, external pressure, and combinations of axial compression and internal or external pressure. Important results are obtained by taking into account prebuckling deformations and stresses induced by edge support. For example, the presence of these deformations and stresses can reduce the axial-compression buckling load of an unpressurized perfect cylinder to 50 percent of the classical value.

INTRODUCTION

Classical theory and experiment are in good agreement for buckling of circular cylindrical shells under uniform external lateral pressure. (See ref. 1.) For external hydrostatic pressure there is similar agreement between experiment and theory except for the lower range of curvature parameter $\left(L^2/rt < 100\right)$, where L, r, and t are the cylinder length, radius, and thickness, respectively. For axial compression, however, severe disagreement exists; experiments have shown that the actual buckling stress for high values of r/t is from 15 to 50 percent of that predicted by classical theory. (See ref. 2.) The disagreement found in hydrostatic pressure tests at low values of the curvature parameter is probably also due to the inability of classical theory to account for axial compression. (See ref. 1.)

Convincing arguments have been made that the occurrence of buckling stresses lower than expected for axial compression is due in part to initial imperfections. For example, the results of large-deflection analysis (ref. 3) have indicated that small initial imperfections can lead to large reductions in the buckling load. However, another potential reason for this disagreement between classical theory and experiment has, until recently, been unexplored. This potential reason is the inconsistent assumption made in classical theory with regard to prebuckling and buckling edge conditions. In classical theory the prebuckling deflection and stress components are assumed to be either constant or zero. Thus, it is implied that the edges of the shell are free until buckling occurs; however, during the buckling process the edges are assumed to be radially restrained (simply supported or clamped).

The effect of one deviation from the classical edge conditions has already been investigated (see refs. 4 and 5) for buckling in axial compression by use of linear equations. The edges of the shell were allowed to remain free during the buckling process and the resulting buckling load was less than half the classical load. Although this result demonstrates effectively the importance of the edge conditions, in practice the occurrence of free edges is rare; the edges of the shell are usually attached to a ring or pressed against the platens of a testing machine. The approach of references 4 and 5 is consistent in the sense that prebuckling and buckling edge conditions are the same. However, it seems more realistic to take the opposite though still consistent approach, wherein from the inception of loading through buckling the edges of the cylinder are radially restrained. Moreover, it is apparent that such restraint must lead to nonuniform prebuckling deflections and stresses throughout the cylinder, the importance of which should be determined. This approach to cylinder buckling analysis has been adopted in the present investigation.

A cylinder without initial imperfections is considered, and large-deflection theory is used to determine the deformations and stresses prior to buckling and to determine the buckling equation. Results are obtained for buckling of simply supported cylinders under axial compression, external pressure, and combinations of axial compression and internal or external pressure. Some results of this investigation were presented in reference 6. The present paper includes the results given in reference 6, some additional results, and a complete discussion of the analysis.

SYMBOLS

C_p	pressure stress coefficient, $\frac{prL^2}{D\pi^2}$
D	plate stiffness, $\frac{Et^3}{12(1 - \mu^2)}$
E	Young's modulus
k_x	axial stress coefficient, $\frac{PL^2}{D\pi^2}$
L	length of cylinder
M	number of stations in half length
N_x, N_y, N_{xy}	in-plane stress resultants
n	number of waves in circumferential direction
P	applied axial in-plane compressive force per unit length
p	pressure
r	radius of cylinder

t thickness of cylinder wall

U,V,W functions of x which appear in the buckling displacements u_B, v_B, and w_B, respectively

u,v,w displacements in the x-, y-, and radial directions, respectively

u_A,w_A prebuckling displacements (functions of x)

u_B,v_B,w_B buckling displacements (functions of x and y)

x,y axial and circumferential directions

Z curvature parameter, $\frac{L^2}{rt}\sqrt{1 - \mu^2}$

$$\nabla^4 = \frac{\partial^4}{\partial x^4} + 2\frac{\partial^4}{\partial x^2 \partial y^2} + \frac{\partial^4}{\partial y^4}$$

$\epsilon_x,\epsilon_y,\gamma_{xy}$ in-plane strains

μ Poisson's ratio

When the subscripts x and y follow a comma, they indicate partial differentiation of the principal symbol with respect to x and y. Primes indicate total derivatives with respect to x.

ANALYSIS

In the large-deflection Donnell theory, the basic differential equations of equilibrium for a cylinder are:

$$\left.\begin{aligned} N_{x,x} + N_{xy,y} &= 0 \\ N_{y,y} + N_{xy,x} &= 0 \\ D\nabla^4 w + \frac{N_y}{r} - \left(N_x w_{,xx} + N_y w_{,yy} + 2N_{xy} w_{,xy}\right) &= p \end{aligned}\right\} \tag{1}$$

According to Hooke's law,

$$\left.\begin{aligned} N_x &= \frac{Et}{1 - \mu^2}\left(\epsilon_x + \mu\epsilon_y\right) \\ N_y &= \frac{Et}{1 - \mu^2}\left(\epsilon_y + \mu\epsilon_x\right) \\ N_{xy} &= \frac{Et}{2(1 + \mu)}\gamma_{xy} \end{aligned}\right\} \tag{2}$$

The nonlinear strain-displacement relations are:

$$\left.\begin{aligned} \epsilon_x &= u,_x + \frac{1}{2} w,_x{}^2 \\ \epsilon_y &= v,_y + \frac{w}{r} + \frac{1}{2} w,_y{}^2 \\ \gamma_{xy} &= u,_y + v,_x + w,_x w,_y \end{aligned}\right\} \tag{3}$$

Equations (1) to (3) provide a complete set of nine equations in the nine unknown stress resultants, strains, and displacements which, together with boundary conditions, specify the problem. The ends of the cylinder are considered to satisfy the following simple support boundary conditions from the initial application of load:

Zero (radial) deflection:

$$w\left(\pm\frac{L}{2}, y\right) = 0 \tag{4a}$$

Zero moment:

$$w,_{xx}\left(\pm\frac{L}{2}, y\right) = 0 \tag{4b}$$

Constant (axial) displacement:

$$u,_y\left(\pm\frac{L}{2}, y\right) = 0 \tag{4c}$$

Zero shear stress:

$$v,_x\left(\pm\frac{L}{2}, y\right) = 0 \tag{4d}$$

It is to be expected that prebuckling deformations are axisymmetric; that is, they are functions only of x and may be obtained directly from equations (1) to (3). If in equations (1) the deformations are functions of x only, then:

$$\left.\begin{aligned} N_{xA}' &= 0 \\ N_{xyA}' &= 0 \\ Dw_A'''' + \frac{1}{r} N_{yA} - N_{xA} w_A'' &= p \end{aligned}\right\} \tag{5}$$

where the subscript A denotes prebuckling values, and the primes denote differentiation with respect to x. The first of equations (5) requires that the prebuckling N_{xA} be constant; thus N_{xA} is set equal to the negative of the compressive load intensity P. The second of equations (5) together with the boundary conditions (4) require that $N_{xyA} = 0$ and $v_A = 0$. Equations (2) and equations (3), if deformations are considered as functions only of x, identify

$$N_{yA} = \frac{Et}{r} w_A - \mu P$$

The equation determining the prebuckling deflection is obtained from equations (5) as:

$$Dw_A'''' + Pw_A'' + \frac{Et}{r^2} w_A = p + \frac{\mu}{r} P \tag{6}$$

Equation (6) has the following solution that satisfies the boundary conditions (4)

$$w_A = A_1 \sin a_1 x \sinh a_2 x + A_2 \cos a_1 x \cosh a_2 x + \frac{r^2}{Et}\left(p + \frac{\mu}{r} P\right) \tag{7}$$

where

$$a_1 = \frac{\pi}{2L}\sqrt{\frac{4\sqrt{3}Z}{\pi^2} + \frac{PL^2}{D\pi^2}}$$

$$a_2 = \frac{\pi}{2L}\sqrt{\frac{4\sqrt{3}Z}{\pi^2} - \frac{PL^2}{D\pi^2}}$$

$$A_1 = \frac{r^2}{Et}\left(p + \frac{\mu}{r} P\right)\frac{\left(a_2^2 - a_1^2\right)\cos\frac{a_1 L}{2}\cosh\frac{a_2 L}{2} - 2a_1 a_2 \sin\frac{a_1 L}{2}\sinh\frac{a_2 L}{2}}{2a_1 a_2\left(\sin^2\frac{a_1 L}{2}\sinh^2\frac{a_2 L}{2} + \cos^2\frac{a_1 L}{2}\cosh^2\frac{a_2 L}{2}\right)}$$

$$A_2 = -\frac{r^2}{Et}\left(p + \frac{\mu}{r} P\right)\frac{\left(a_2^2 - a_1^2\right)\sin\frac{a_1 L}{2}\sinh\frac{a_2 L}{2} + 2a_1 a_2 \cos\frac{a_1 L}{2}\cosh\frac{a_2 L}{2}}{2a_1 a_2\left(\sin^2\frac{a_1 L}{2}\sinh^2\frac{a_2 L}{2} + \cos^2\frac{a_1 L}{2}\cosh^2\frac{a_2 L}{2}\right)}$$

With w_A known, the axisymmetric prebuckling axial displacement u_A can be found from equations (2) and (3). A solution to the axisymmetric problem was first obtained in reference 7 and is reported in reference 8.

To the prebuckling displacements are added the infinitesimal nonaxisymmetric displacements u_B, v_B, and w_B that occur at buckling:

$$\left.\begin{aligned} u &= u_A(x) + u_B(x,y) \\ v &= v_B(x,y) \\ w &= w_A(x) + w_B(x,y) \end{aligned}\right\} \tag{8}$$

The displacements u_B, v_B, and w_B must also satisfy simple-support boundary conditions consistent with the axisymmetric prebuckling solution. The following buckling equations may now be obtained by substituting equations (8) into equations (1) to (3), subtracting out identities (5) relating subscript A deformations, and then neglecting terms nonlinear with respect to subscript B deformations:

$$\left.\begin{aligned} u_{B,xx} + \frac{1-\mu}{2} u_{B,yy} + \frac{1+\mu}{2} v_{B,xy} + \frac{\mu}{r} w_{B,x} + \left(w_A' w_{B,x}\right)_{,x} + \frac{1-\mu}{2} w_A' w_{B,yy} &= 0 \\ \frac{1+\mu}{2} u_{B,xy} + v_{B,yy} + \frac{1-\mu}{2} v_{B,xx} + \frac{1}{r} w_{B,y} + \frac{1-\mu}{2} w_A'' w_{B,y} + \frac{1+\mu}{2} w_A' w_{B,xy} &= 0 \\ D\nabla^4 w_B + \frac{1}{r} N_{yB} + P w_{B,xx} + \left(\mu P - \frac{Et}{r} w_A\right) w_{B,yy} - w_A'' N_{xB} &= 0 \end{aligned}\right\} \quad (9)$$

where

$$N_{xB} = \frac{Et}{1-\mu^2}\left[u_{B,x} + w_A' w_{B,x} + \mu\left(v_{B,y} + \frac{w_B}{r}\right)\right]$$

$$N_{yB} = \frac{Et}{1-\mu^2}\left[v_{B,y} + \frac{w_B}{r} + \mu\left(u_{B,x} + w_A' w_{B,x}\right)\right]$$

The conditions of continuity around the cylinder are satisfied if

$$\left.\begin{aligned} u_B &= U(x)\sin\frac{ny}{r} \\ v_B &= V(x)\cos\frac{ny}{r} \\ w_B &= W(x)\sin\frac{ny}{r} \end{aligned}\right\} \quad (10)$$

where n, the number of waves around the cylinder, is an integer. Equations (9) may now be converted to the following ordinary differential equations relating U, V, and W which have complicated variable coefficients and which are not solved here but are included only for the sake of completeness:

$$\left.\begin{aligned} U'' - \frac{1-\mu}{2}\frac{n^2}{r^2} U - \frac{1+\mu}{2}\frac{n}{r} V' + \frac{\mu}{r} W' + \left(w_A' W'\right)' - \frac{1-\mu}{2}\frac{n^2}{r^2} w_A' W &= 0 \\ \frac{1+\mu}{2}\frac{n}{r} U' - \frac{n^2}{r^2} V + \frac{1-\mu}{2} V'' + \frac{n}{r^2} W + \frac{1-\mu}{2}\frac{n}{r} w_A'' W + \frac{1+\mu}{2}\frac{n}{r} w_A' W' &= 0 \\ D\left(W'''' - 2\frac{n^2}{r^2} W'' + \frac{n^4}{r^4} W\right) + \frac{1}{r}\bar{N}_{yB} + P W'' - \left(\mu P - \frac{Et}{r} w_A\right)\frac{n^2}{r^2} W - w_A'' \bar{N}_{xB} &= 0 \end{aligned}\right\} \quad (11)$$

where

$$\bar{N}_{xB} = \frac{Et}{1 - \mu^2}\left[U' + w_A'W' + \mu\left(-\frac{n}{r}V + \frac{1}{r}W\right)\right]$$

$$\bar{N}_{yB} = \frac{Et}{1 - \mu^2}\left[-\frac{n}{r}V + \frac{1}{r}W + \mu\left(U' + w_A'W'\right)\right]$$

Instead of solving these equations directly, an equivalent energy method was used. The potential energy Π of the loaded cylinder is

$$\Pi = \frac{Et}{2(1 - \mu^2)}\int_{-L/2}^{L/2}\int_0^{2\pi r}\left(\epsilon_x^2 + \epsilon_y^2 + 2\mu\epsilon_x\epsilon_y + \frac{1 - \mu}{2}\gamma_{xy}^2\right)dy\,dx$$

$$+ \frac{D}{2}\int_{-L/2}^{L/2}\int_0^{2\pi r}\left[w_{,xx}^2 + w_{,yy}^2 + 2\mu w_{,xx}w_{,yy} + 2(1 - \mu)w_{,xy}^2\right]dy\,dx \quad (12)$$

When the first variation of this potential energy expression, in which equations (3) are used for the definition of the strains, is taken with respect to u, v, and w and set equal to zero, equations (1) in terms of u, v, and w result. Noting that $-P = \frac{Et}{1 - \mu^2}\left(u_{A,x} + \frac{1}{2}w_A'^2 + \frac{\mu}{r}w_A\right)$, equations (3) for the strains in terms of the u, v, and w of equations (8) are

$$\left.\begin{aligned}
\epsilon_x &= -\left(1 - \mu^2\right)\frac{P}{Et} - \frac{\mu}{r}w_A + u_{B,x} + w_A'w_{B,x} + \frac{1}{2}w_{B,x}^2 \\
\epsilon_y &= \frac{1}{r}w_A + v_{B,y} + \frac{1}{r}w_B + \frac{1}{2}w_{B,y}^2 \\
\gamma_{xy} &= v_{B,x} + u_{B,y} + w_A'w_{B,y} + w_{B,x}w_{B,y}
\end{aligned}\right\} \quad (13)$$

When equations (13) are used for the definition of the strains in the energy expression (12), y dependence can be eliminated if upon substitution from equations (10) the y integration is performed. It is also convenient at this point to drop all terms of higher than second degree in U, V, and W (so that the resulting expression corresponds to eqs. (11)). Thus, the potential-energy function which is to be minimized is

$$\Pi = \frac{Et\pi r}{2(1-\mu^2)} \int_{-L/2}^{L/2} \left\{ 2\left[(1-\mu^2)\frac{P}{Et} + \frac{\mu}{r} w_A\right]^2 + (U' + w_A'W')^2 - \left[(1-\mu^2)\frac{P}{Et} \right.\right.$$

$$\left. + \frac{\mu}{r} w_A\right]\left(W'^2 + \frac{4\mu}{r} w_A + \frac{\mu n^2}{r^2} W^2\right) + \frac{2}{r^2} w_A^2 + \left(\frac{1}{r} W - \frac{n}{r} V\right)^2 + \frac{n^2}{r^3} w_A W^2$$

$$+ 2\mu(U' + w_A'W')\left(\frac{1}{r} W - \frac{n}{r} V\right) + \frac{\mu}{r} w_A W'^2 + \frac{1-\mu}{2}\left(V' + \frac{n}{r} U + \frac{n}{r} w_A'W\right)^2 \Bigg\} dx$$

$$+ \frac{D\pi r}{2} \int_{-L/2}^{L/2} \left[2w_A''^2 + W''^2 + \frac{n^4}{r^4} W^2 - 2\mu \frac{n^2}{r^2} WW'' + 2(1-\mu)\frac{n^2}{r^2} W'^2 \right] dx \qquad (14)$$

When the derivatives occurring in the expression for Π are replaced by finite differences and the integrations are replaced by finite sums, the minimization process leads directly to a set of simultaneous linear algebraic equations for the U, V, and W values at discrete points along the length of the cylinder. The stations along the length of the cylinder are taken to be equally spaced and numbered from $m = 0$ at the center to $m = M$ at the end. There are also stations corresponding to $m = -1$ and $m = M + 1$. The following difference approximations for the first and second derivatives are used:

$$\left(\frac{df}{dx}\right)_{m+\frac{1}{2}} = \frac{f_{m+1} - f_m}{\epsilon}$$

$$\left(\frac{d^2 f}{dx^2}\right)_m = \frac{f_{m+1} - 2f_m + f_{m-1}}{\epsilon^2}$$

where m indicates the station and ϵ is the distance between stations. Integrals are approximated by finite sums according to the trapezoidal rule. The quantities U and W are evaluated at the full stations; V is evaluated at the half stations. When these replacements are carried out, equation (14) becomes

$$\Pi = \frac{Et\pi r\epsilon}{1-\mu^2}\sum_{m=0}^{M-1}\Bigg\{2\left[\left(1-\mu^2\right)\frac{P}{Et}+\frac{\mu}{r}\,w_{A_{m+\frac{1}{2}}}\right]^2+\left(\frac{U_{m+1}-U_m}{\epsilon}+w'_{A_{m+\frac{1}{2}}}\,\frac{W_{m+1}-W_m}{\epsilon}\right)^2$$

$$-\left[\left(1-\mu^2\right)\frac{P}{Et}+\frac{\mu}{r}\,w_{A_{m+\frac{1}{2}}}\right]\left[\left(\frac{W_{m+1}-W_m}{\epsilon}\right)^2+4\,\frac{\mu}{r}\,w_{A_{m+\frac{1}{2}}}+\mu\,\frac{n^2}{r^2}\left(\frac{W_{m+1}+W_m}{2}\right)^2\right]$$

$$+\frac{2}{r^2}\,w^2_{A_{m+\frac{1}{2}}}+\left(\frac{W_{m+1}+W_m}{2r}-\frac{n}{r}\,V_{m+\frac{1}{2}}\right)^2+\frac{n^2}{r^3}\,w_{A_{m+\frac{1}{2}}}\left(\frac{W_{m+1}+W_m}{2}\right)^2+2\mu\left(\frac{U_{m+1}-U_m}{\epsilon}\right.$$

$$\left.+w'_{A_{m+\frac{1}{2}}}\,\frac{W_{m+1}-W_m}{\epsilon}\right)\left(\frac{W_{m+1}+W_m}{2r}-\frac{n}{r}\,V_{m+\frac{1}{2}}\right)+\frac{\mu}{r}\,w_{A_{m+\frac{1}{2}}}\left(\frac{W_{m+1}-W_m}{\epsilon}\right)^2\Bigg\}$$

$$+\frac{Et\pi r\epsilon}{2(1+\mu)}\sum_{m=0}^{M}\left[1-\frac{1}{2}\left(\delta_{mo}+\delta_{mM}\right)\right]\left(\frac{V_{m+\frac{1}{2}}-V_{m-\frac{1}{2}}}{\epsilon}+\frac{n}{r}\,U_m+w'_{A_m}\,\frac{n}{r}\,W_m\right)^2$$

$$+D\pi r\epsilon\sum_{m=0}^{M}\left[1-\frac{1}{2}\left(\delta_{mo}+\delta_{mM}\right)\right]\left[2w''^2_{A_m}+\left(\frac{W_{m+1}-2W_m+W_{m-1}}{\epsilon^2}\right)^2+\frac{n^4}{r^4}\,W_m^2\right.$$

$$\left.-2\mu\,\frac{n^2}{r^2}\,W_m\left(\frac{W_{m+1}-2W_m+W_{m-1}}{\epsilon^2}\right)\right]+2D\pi r\epsilon(1-\mu)\sum_{m=0}^{M-1}\frac{n^2}{r^2}\left(\frac{W_{m+1}-W_m}{\epsilon}\right)^2 \qquad (15)$$

where δ_{mo} and δ_{mM} are Kronecker deltas which have the value zero if the subscripts differ in value or have the value unity if the subscripts are the same.

The deflections are assumed to be symmetric about the center of the cylinder; therefore, at $x = 0$ the geometric conditions are $U = V' = W' = 0$ or

$$\left.\begin{aligned} U_0 &= 0 \\ V_{-i/2} &= V_{1/2} \\ W_{-1} &= W_1 \end{aligned}\right\} \qquad (16)$$

At $x = \frac{L}{2} = M\epsilon$, the geometric conditions that correspond to equations (4) are $U = V' = W = 0$ or

$$\left.\begin{aligned} U_M &= 0 \\ V_{M-\frac{1}{2}} &= V_{M+\frac{1}{2}} \\ W_M &= 0 \end{aligned}\right\} \tag{17}$$

According to the minimum potential-energy method for this case, the following equations subject to the foregoing conditions (eqs. (16) and (17)) must be satisfied

$$\left.\begin{aligned} \frac{\partial \Pi}{\partial U_m} &= 0 \qquad (m = 1, 2, \ldots, M-1) \\ \frac{\partial \Pi}{\partial V_{m+\frac{1}{2}}} &= 0 \qquad (m = 0, 1, \ldots, M-1) \\ \frac{\partial \Pi}{\partial W_m} &= 0 \qquad (m = 0, 1, \ldots, M-1, M+1) \end{aligned}\right\} \tag{18}$$

The $(M + 1)$ equation of the last set provides for automatic satisfaction of the natural boundary condition: zero moment at $x = \frac{L}{2}$. Thus,

$$W_{M+1} = -W_{M-1}$$

and W_{M+1} can be eliminated as one of the unknowns to leave $3M - 1$ unknowns

$$U_1, U_2, \ldots, U_{M-1}; V_{1/2}, V_{3/2}, \ldots, V_{M-\frac{1}{2}}; W_0, W_1, \ldots, W_{M-1}$$

The equations obtained are homogeneous in the $3M - 1$ unknowns, so that either all the unknowns are zero or the following determinant of the matrix of coefficients is zero

$$\begin{vmatrix} A_{11} & A_{12} & A_{13} \\ A_{21} & A_{22} & A_{23} \\ A_{31} & A_{32} & A_{33} \end{vmatrix} = 0 \tag{19}$$

This determinant is symmetric about the principal diagonal (A_{11}, A_{22}, and A_{33} are symmetric submatrices; A_{21}, A_{31}, and A_{32} are the transposes of A_{12}, A_{13}, and A_{23}, respectively), and the submatrices have the following sets of numbers which are of order indicated:

$$A_{11} = \begin{bmatrix} 2+\frac{1-\mu}{2}\left(\frac{nL}{2Mr}\right)^2 & -1 & 0 & \cdots & & 0 \\ -1 & 2+\frac{1-\mu}{2}\left(\frac{nL}{2Mr}\right)^2 & -1 & 0 & \cdots & 0 \\ 0 & -1 & 2+\frac{1-\mu}{2}\left(\frac{nL}{2Mr}\right)^2 & -1 & 0 \cdots & 0 \\ & & \ddots & & & \\ 0 & \cdots & & 0 & -1 & 2+\frac{1-\mu}{2}\left(\frac{nL}{2Mr}\right)^2 \end{bmatrix}$$

$(M-1)\times(M-1)$

$$A_{12} = \begin{bmatrix} -\frac{1+\mu}{2}\frac{nL}{2Mr} & \frac{1+\mu}{2}\frac{nL}{2Mr} & 0 & \cdots & 0 \\ 0 & -\frac{1+\mu}{2}\frac{nL}{2Mr} & \frac{1+\mu}{2}\frac{nL}{2Mr} & 0 \cdots & 0 \\ & & \ddots & & \\ 0 & \cdots & 0 & -\frac{1+\mu}{2}\frac{nL}{2Mr} & \frac{1+\mu}{2}\frac{nL}{2Mr} \end{bmatrix}$$

$(M-1)\times M$

$$A_{13} = \begin{bmatrix} \frac{\mu}{4M}-w_A'\left(\frac{1}{4M}\right) & w_A'\left(\frac{1}{4M}\right)+w_A'\left(\frac{3}{4M}\right) + \frac{1-\mu}{2}\left(\frac{nL}{2Mr}\right)^2 w_A'\left(\frac{1}{2M}\right) & -\frac{\mu}{4M}-w_A'\left(\frac{3}{4M}\right) & 0 & \cdots & 0 \\ 0 & \frac{\mu}{4M}-w_A'\left(\frac{3}{4M}\right) & w_A'\left(\frac{3}{4M}\right)+w_A'\left(\frac{5}{4M}\right) + \frac{1-\mu}{2}\left(\frac{nL}{2Mr}\right)^2 w_A'\left(\frac{1}{M}\right) & -\frac{\mu}{4M}-w_A'\left(\frac{5}{4M}\right) & 0 \cdots & 0 \\ & & \ddots & & & \\ 0 & \cdots & 0 & \frac{\mu}{4M}-w_A'\left(\frac{1}{2}-\frac{5}{4M}\right) & w_A'\left(\frac{1}{2}-\frac{5}{4M}\right)+w_A'\left(\frac{1}{2}-\frac{3}{4M}\right) + \frac{1-\mu}{2}\left(\frac{nL}{2Mr}\right)^2 w_A'\left(\frac{1}{2}-\frac{1}{M}\right) & -\frac{\mu}{2M}-w_A'\left(\frac{1}{2}-\frac{3}{4M}\right) \\ 0 & \cdots & & 0 & \frac{\mu}{4M}-w_A'\left(\frac{1}{2}-\frac{3}{4M}\right) & w_A'\left(\frac{1}{2}-\frac{3}{4M}\right)+w_A'\left(\frac{1}{2}-\frac{1}{4M}\right) + \frac{1-\mu}{2}\left(\frac{nL}{2Mr}\right)^2 w_A'\left(\frac{1}{2}-\frac{1}{2M}\right) \end{bmatrix}$$

$(M-1)\times M$

$$A_{22} = \begin{bmatrix} \left(\frac{nL}{2Mr}\right)^2+\frac{1-\mu}{2} & -\frac{1-\mu}{2} & 0 & \cdots & & 0 \\ -\frac{1-\mu}{2} & \left(\frac{nL}{2Mr}\right)^2+\frac{1-\mu}{2} & -\frac{1-\mu}{2} & 0 & \cdots & 0 \\ 0 & -\frac{1-\mu}{2} & \left(\frac{nL}{2Mr}\right)^2+\frac{1-\mu}{2} & -\frac{1-\mu}{2} & 0 & \cdots \\ & & \ddots & & & \\ 0 & \cdots & & 0 & -\frac{1-\mu}{2} & \left(\frac{nL}{2Mr}\right)^2+\frac{1-\mu}{2} \end{bmatrix}_{M \times M}$$

$$A_{23} = \begin{bmatrix} \frac{nL}{2Mr}\left[-\frac{1}{4M}+\mu w_A'\left(\frac{1}{4M}\right)\right. & \frac{nL}{2Mr}\left[-\frac{1}{2M}-\mu w_A'\left(\frac{1}{4M}\right)\right. & 0 & \cdots & 0 \\ & \left.-\frac{1-\mu}{2}w_A'\left(\frac{1}{2M}\right)\right] & & & \\ 0 & \frac{nL}{2Mr}\left[-\frac{1}{4M}+\mu w_A'\left(\frac{3}{4M}\right)\right. & \frac{nL}{2Mr}\left[-\frac{1}{4M}-\mu w_A'\left(\frac{3}{4M}\right)\right. & 0 & \cdots & 0 \\ & \left.+\frac{1-\mu}{2}w_A'\left(\frac{1}{2M}\right)\right] & \left.-\frac{1-\mu}{2}w_A'\left(\frac{1}{M}\right)\right] & & & \\ & & \ddots & & & \\ 0 & \cdots & 0 & \frac{nL}{2Mr}\left[-\frac{1}{4M}+\mu w_A'\left(\frac{1}{2}-\frac{3}{4M}\right)\right. & \frac{nL}{2Mr}\left[-\frac{1}{4M}-\mu w_A'\left(\frac{1}{2}-\frac{3}{4M}\right)\right. \\ & & & \left.+\frac{1-\mu}{2}w_A'\left(\frac{1}{2}-\frac{1}{M}\right)\right] & \left.-\frac{1-\mu}{2}w_A'\left(\frac{1}{2}-\frac{1}{2M}\right)\right] \\ 0 & \cdots & & 0 & \frac{nL}{2Mr}\left[-\frac{1}{4M}+\mu w_A'\left(\frac{1}{2}-\frac{1}{4M}\right)\right. \\ & & & & \left.+\frac{1-\mu}{2}w_A'\left(\frac{1}{2}-\frac{1}{2M}\right)\right] \end{bmatrix}_{M \times M}$$

$$A_{33} = \begin{bmatrix} a_{00} & a_{01} & \frac{(1-\mu^2)M^2}{3Z^2} & 0 & \cdots & & 0 \\ a_{01} & a_{11} & a_{12} & \frac{(1-\mu^2)M^2}{3Z^2} & 0 & \cdots & 0 \\ \frac{(1-\mu^2)M^2}{3Z^2} & a_{12} & a_{22} & a_{23} & \frac{(1-\mu^2)M^2}{3Z^2} & 0 & \cdots & 0 \\ & & & \ddots & & & \\ 0 & \cdots & 0 & \frac{(1-\mu^2)M^2}{3Z^2} & a_{M-4,M-3} & a_{M-3,M-3} & a_{M-3,M-2} & \frac{(1-\mu^2)M^2}{3Z^2} \\ 0 & \cdots & & 0 & \frac{(1-\mu^2)M^2}{3Z^2} & a_{M-3,M-2} & a_{M-2,M-2} & a_{M-2,M-1} \\ 0 & \cdots & & & 0 & \frac{(1-\mu^2)M^2}{3Z^2} & a_{M-2,M-1} & a_{M-1,M-1} \end{bmatrix}_{M \times M}$$

where

$$a_{00} = \left[w_A'\left(\frac{1}{4M}\right)\right]^2 + \frac{1}{16M^2} - \frac{PL^2(1-\mu^2)}{12DZ^2} + \frac{1-\mu^2}{4}\left(\frac{nL}{2Mr}\right)^2\left[w_A\left(\frac{1}{4M}\right) + \frac{prL^2}{12DZ^2}\right]$$

$$- \frac{\mu}{2M} w_A'\left(\frac{1}{4M}\right) + \frac{(1-\mu^2)M^2}{3Z^2}\left[3 + 2\left(\frac{nL}{2Mr}\right)^2 + \frac{1}{2}\left(\frac{nL}{2Mr}\right)^4\right]$$

$$a_{01} = -\left[w_A'\left(\frac{1}{4M}\right)\right]^2 + \frac{1}{16M^2} + \frac{PL^2(1-\mu^2)}{12DZ^2} + \frac{1-\mu^2}{4}\left(\frac{nL}{2Mr}\right)^2\left[w_A\left(\frac{1}{4M}\right) + \frac{prL^2}{12DZ^2}\right]$$

$$- \frac{(1-\mu^2)M^2}{3Z^2}\left[4 + 2\left(\frac{nL}{2Mr}\right)^2\right]$$

$$a_{11} = \left[w_A'\left(\frac{1}{4M}\right)\right]^2 + \left[w_A'\left(\frac{3}{4M}\right)\right]^2 + \frac{1}{8M^2} - \frac{PL^2(1-\mu^2)}{6DZ^2} + \frac{1-\mu^2}{4}\left(\frac{nL}{2Mr}\right)^2\left[w_A\left(\frac{1}{4M}\right) + w_A\left(\frac{3}{4M}\right)\right.$$

$$\left. + \frac{prL^2}{6DZ^2}\right] + \frac{1-\mu}{2}\left(\frac{nL}{2Mr}\right)^2\left[w_A'\left(\frac{1}{2M}\right)\right]^2 + \frac{\mu}{2M}\left[w_A'\left(\frac{1}{4M}\right) - w_A'\left(\frac{3}{4M}\right)\right]$$

$$+ \frac{(1-\mu^2)M^2}{3Z^2}\left[7 + 4\left(\frac{nL}{2Mr}\right)^2 + \left(\frac{nL}{2Mr}\right)^4\right]$$

$$a_{12} = -\left[w_A'\left(\frac{3}{4M}\right)\right]^2 + \frac{1}{16M^2} + \frac{PL^2(1-\mu^2)}{12DZ^2} + \frac{1-\mu^2}{4}\left(\frac{nL}{2Mr}\right)^2\left[w_A\left(\frac{3}{4M}\right) + \frac{prL^2}{12DZ^2}\right]$$

$$- \frac{(1-\mu^2)M^2}{3Z^2}\left[4 + 2\left(\frac{nL}{2Mr}\right)^2\right]$$

$$a_{mm} = \left[w_A'\left(\frac{2m-1}{4M}\right)\right]^2 + \left[w_A'\left(\frac{2m+1}{4M}\right)\right]^2 + \frac{1}{8M^2} - \frac{PL^2(1-\mu^2)}{6DZ^2} + \frac{1-\mu^2}{4}\left(\frac{nL}{2Mr}\right)^2\left[w_A\left(\frac{2m-1}{4M}\right)\right.$$

$$\left. + w_A\left(\frac{2m+1}{4M}\right) + \frac{prL^2}{6DZ^2}\right] + \frac{1-\mu}{2}\left(\frac{nL}{2Mr}\right)^2\left[w_A'\left(\frac{m}{2M}\right)\right]^2 + \frac{\mu}{2M}\left[w_A'\left(\frac{2m-1}{4M}\right) - w_A'\left(\frac{2m+1}{4M}\right)\right]$$

$$+ \frac{(1-\mu^2)M^2}{3Z^2}\left[6 + 4\left(\frac{nL}{2Mr}\right)^2 + \left(\frac{nL}{2Mr}\right)^4\right] \qquad (m = 2, 3, \ldots, M-2)$$

$$a_{m,m+1} = -\left[w_A'\left(\frac{2m+1}{4M}\right)\right]^2 + \frac{1}{16M^2} + \frac{PL^2(1-\mu^2)}{12DZ^2} + \frac{1-\mu^2}{4}\left(\frac{nL}{2Mr}\right)^2\left[w_A\left(\frac{2m+1}{4M}\right) + \frac{prL^2}{12DZ^2}\right]$$

$$- \frac{(1-\mu^2)M^2}{3Z^2}\left[4 + 2\left(\frac{nL}{2Mr}\right)^2\right]$$

$$(m = 2, 3, \ldots, M-2)$$

$$a_{M-1,M-1} = \left[w_A'\left(\frac{2M-3}{4M}\right)\right]^2 + \left[w_A'\left(\frac{2M-1}{4M}\right)\right]^2 + \frac{1}{8M^2} - \frac{PL^2(1-\mu^2)}{6DZ^2}$$

$$+ \frac{1-\mu^2}{4}\left(\frac{nL}{2Mr}\right)^2\left[w_A\left(\frac{2M-3}{4M}\right) + w_A\left(\frac{2M-5}{4M}\right) + \frac{prL^2}{6DZ^2}\right] + \frac{1-\mu}{2}\left(\frac{nL}{2Mr}\right)^2\left[w_A'\left(\frac{M-1}{2M}\right)\right]^2$$

$$+ \frac{\mu}{2M}\left[w_A'\left(\frac{2M-3}{4M}\right) - w_A'\left(\frac{2M-1}{4M}\right)\right] + \frac{(1-\mu^2)M^2}{3Z^2}\left[5 + 4\left(\frac{nL}{2Mr}\right)^2 + \left(\frac{nL}{2Mr}\right)^4\right]$$

The argument of w_A and its derivatives in the previous expressions is in the dimensionless form x/L (instead of x).

When the number of waves around the cylinder $nL/\pi r$, the number of stations in a half length M, the cylinder of interest Z, the internal pressure $prL^2/D\pi^2$, and the Poisson's ratio μ for the material ($\mu = 1/3$ in the present calculation) are chosen, the requirement that the determinant vanishes provides the desired eigenvalue $\left(\frac{PL^2}{D\pi^2}\right)$ for buckling. The correct choices of n and M are discussed in the following section.

LIMITATIONS OF THE CALCULATIONS

If accurate results are to be obtained, the value of M must be large enough to provide about four stations for each prebuckling (inward or outward) wrinkle. In the present calculation at least four and usually five or more stations were provided per wrinkle. For $Z > 1{,}000$, this criterion led to equations involving determinants that were too large for economical application of the IBM 7090 computing machine used. Hence, calculations have been limited to $Z \leqq 1{,}000$. For the presented results: $M = 17$ for $Z \leqq 200$, $M = 34$ for $Z = 500$, and $M = 50$ for $Z = 1{,}000$.

The proper value of n is the integral value which yields the lowest buckling load, with the physical restriction that n cannot be less than 2 (since $n = 1$ is simple translation and $n = 0$ is an axisymmetric form). Little accuracy is lost, however, if n is considered to be continuously variable for $n > 2$. It was found that $n = 2$ gave the condition for instability for almost every case except for the range of higher external pressures. The differential equations of equilibrium (eqs. (1)) are accurate for the case $n = 2$ only if at least three wrinkles are present in every part of a cylinder length equal to the

radius so that the deformations are extensional. (See ref. 9.) For this reason small values of the curvature parameter ($Z < 50$) could not be treated for axial compression and for combinations of axial compression and internal pressure.

RESULTS

In figures 1 to 4 interaction curves are presented for values of the curvature parameter $Z = 50$, 100, 200, and 500. Each point on the curve presents a combination of axial compression and lateral pressure that causes buckling. When the curves depend on r/t, they correspond to $n = 2$; elsewhere, the results were given by $n > 2$ with n assumed continuously variable. At the end points to the left the curves give the buckling pressures for cylinders under external lateral pressure alone. The hydrostatic pressure for buckling is given by the point on the curve marked by a cross. When the pressure is zero, note that the axial buckling stress is 50 percent or less of the classical value. With internal pressure present, the axial stress required for buckling increases until it approaches the classical value. Stress coefficients for external lateral pressure alone, external hydrostatic pressure alone, and axial compression alone are presented in figures 5, 6, and 7, respectively, for a wide range of curvature parameter Z (within the limitations specified in the previous section).

DISCUSSION

Experimental results are available in reference 10 for cylinders with combinations of internal pressure and axial compression and with curvature parameters about equal to those presented in figures 1 and 4. The experimentally obtained buckling stress coefficients are plotted along with the theoretical curves in figures 1 and 4. A comparison of the results shows that, although the experimental cylinders were ring supported and the theory was for simply supported cylinders, there is much better quantitative agreement of experiment with present theory than with classical theory. The evident disagreement in the shapes of the theoretical and experimental interaction curves has not been explained.

It should be noted that the boundary conditions on inplane buckling displacements of the present theory $u_{B,y}\left(\pm\frac{L}{2},y\right) = v_{B,x}\left(\pm\frac{L}{2},y\right) = 0$ are different from the corresponding boundary conditions of the classical theory $u_{B,x}\left(\pm\frac{L}{2},y\right) = v_{B}\left(\pm\frac{L}{2},y\right) = 0$. In classical theory essentially the same results are obtained for both sets of inplane boundary conditions for cylinders in axial compression and internal pressure. Recently Fischer obtained results on essentially the same basis as that of the present paper except that he satisfied the classical inplane conditions. (See ref. 11.) He obtained markedly different results - much smaller changes from the classical theory - which indicates that the buckling load of a cylinder in axial compression is quite sensitive to inplane boundary conditions.

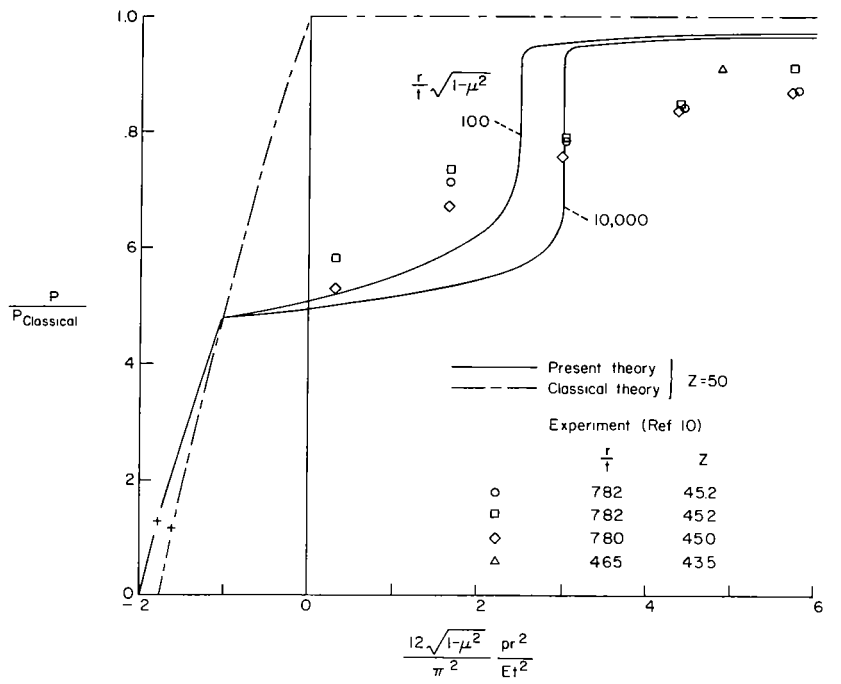

Figure 1.- Theoretical and experimental results for buckling of a cylinder of low Z under combinations of axial compression and internal pressure. Crosses indicate hydrostatic external pressure for buckling.

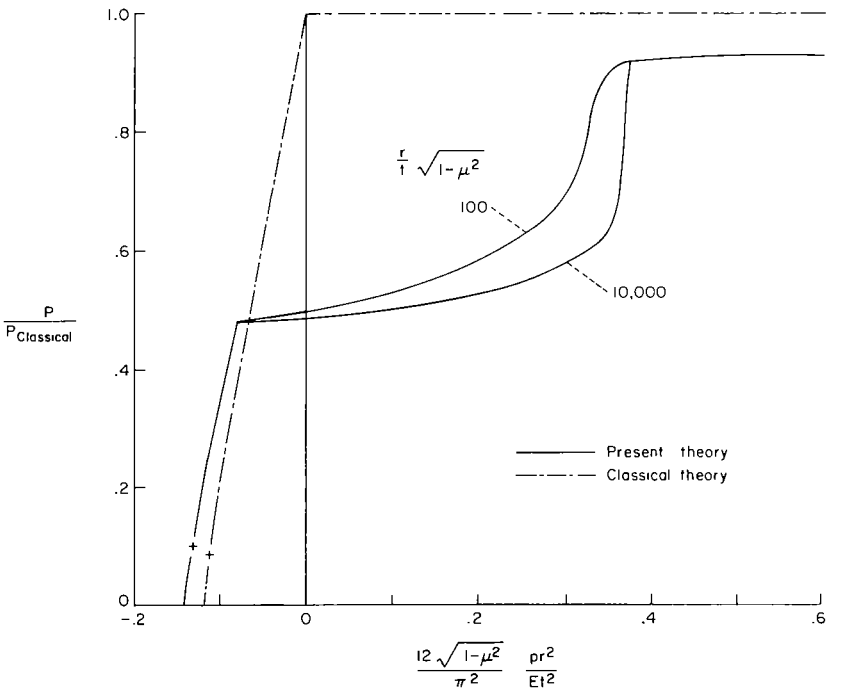

Figure 2.- Theoretical results for buckling of a cylinder of Z = 100 under combinations of axial compression and internal pressure. Crosses indicate hydrostatic external pressure for buckling.

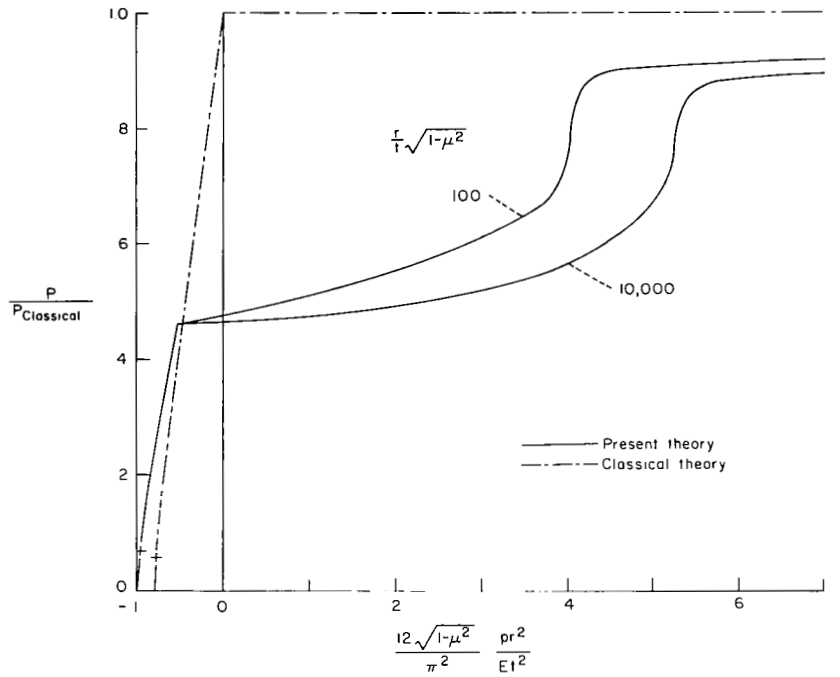

Figure 3.- Theoretical results for buckling of a cylinder of Z = 200 under combinations of axial compression and internal pressure. Crosses indicate hydrostatic external pressure for buckling.

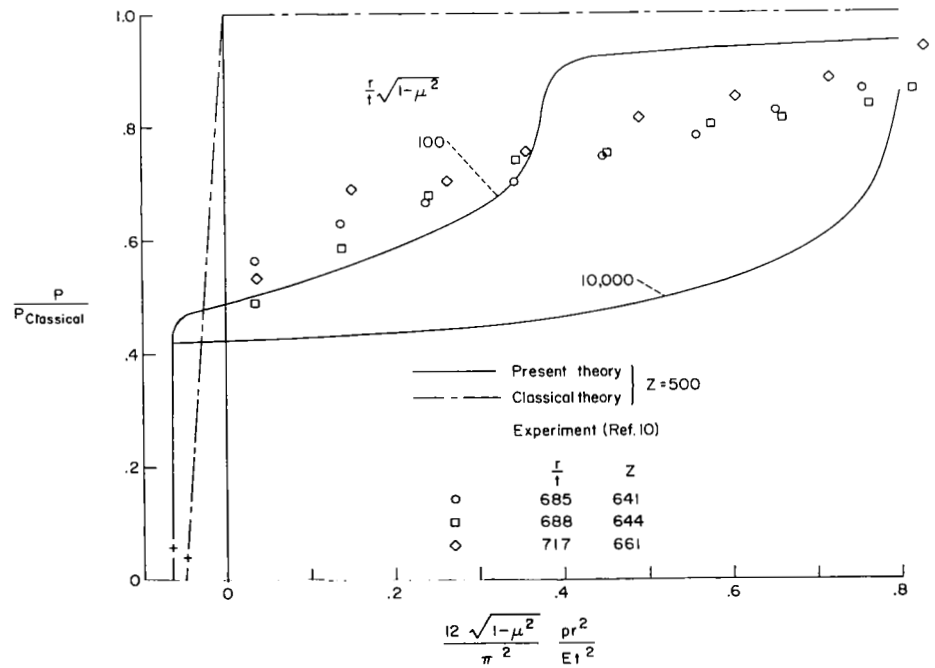

Figure 4.- Theoretical and experimental results for buckling of a cylinder of high Z under combinations of axial compression and internal pressure. Crosses indicate hydrostatic external pressure for buckling.

In figure 5 the end points of the curves of figures 1 to 4, as well as some additional calculated results for external lateral pressure, are plotted against the curvature parameter Z, together with the corresponding classical curve and with experimental data. Comparison of the theoretical results shows that the prebuckling stresses and deflections and the different boundary conditions serve to stiffen the cylinders by about 25 percent at higher values of Z. In the range of lower Z this stiffening effect disappears. Classical theory agrees better with experiment than the present theory.

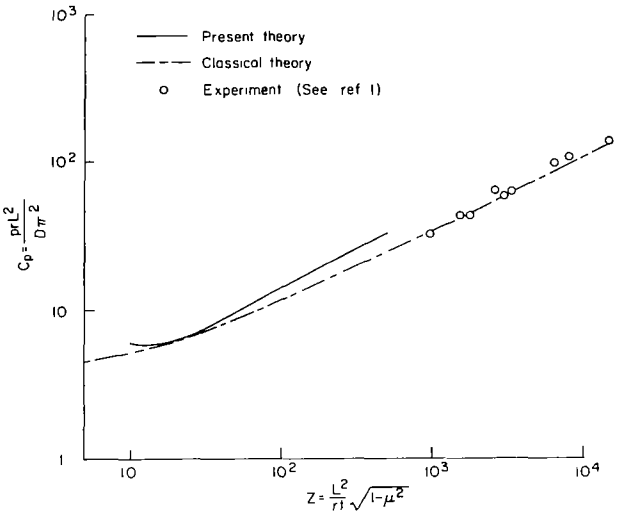

Figure 5.- Theoretical and experimental results for buckling of cylinders under lateral pressure.

In figure 6 results of the present theory for external hydrostatic pressure are plotted against the curvature parameter Z, together with the corresponding classical curve and with experiment. Comparison of the theoretical results shows that prebuckling stresses and deformations and the different inplane boundary conditions serve to stiffen the cylinder by about 25 percent for higher values of Z. In the range of lower Z this stiffening effect disappears and prebuckling stresses and deformations serve to weaken the cylinder to about 80 percent of the classical value. Thus, whereas the classical theory agrees with experiment in the range of higher values of Z and disagrees in the range of lower values of Z, the present results follow the trend of experiment and yield buckling pressures roughly 25 percent high in both regions.

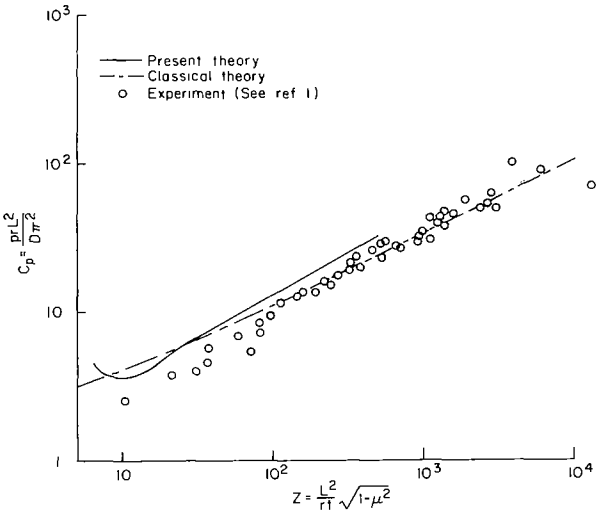

Figure 6.- Theoretical and experimental results for buckling of cylinders under hydrostatic pressure.

For axial compression of unpressurized cylinders the present results are more than 50 percent below the classical values. (See fig. 7.) Thus, the axial buckling load is sensitive to the prebuckling deformations and stresses resulting from restraint of the edges. The value of the buckling load from the present theory is dependent on radius-thickness ratio, whereas in the classical theory it is not. The dependence on radius-thickness ratio occurs when the critical wave form is determined to have two waves in the circumferential direction, and it can be seen from figure 7 that the empirical curves of reference 2 - and therefore experimental results - exhibit stronger dependence on radius-thickness ratio. Agreement between theoretical and empirical curves is much better with the present theory than with classical theory, especially for low radius-thickness ratios.

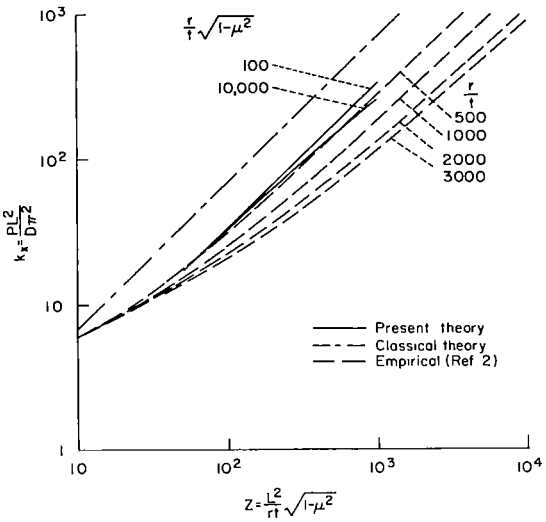

Figure 7.- Theoretical and empirical results for buckling of cylinders in axial compression.

Neither the results of the present theory nor the results of classical theory for buckling in axial compression indicate that the buckle wave form is of the diamond pattern as indicated by buckled experimental cylinders. The results of present theory, which specify two waves in the circumferential direction at buckling, deviate even farther from the experimental buckled wave form than the results of classical theory. However, previous work has shown (see ref. 12) that the equilibrium configuration of a structure corresponding to the mode at buckling need not be stable under many conditions of loading. If the buckling mode is not stable, it might not necessarily resemble the final shape of a buckled experimental structure.

CONCLUDING REMARKS

The present paper has focused attention on a serious shortcoming of classical buckling theory. In the interest of avoiding complicated prebuckling deformations and stresses, the classical approach is to relax completely the supports in the prebuckling range and thus to assume that the prebuckling stresses are zero or constant and that the prebuckling deformations are zero, constant, or linear. Prebuckling deformations and stresses due to edge support have been ignored also in studies of effects of initial imperfections. In every practical cylindrical shell structure, however, some measure of radial support is present from the beginning of loading so that, prior to buckling, complicated axisymmetric deformations and stresses are present to modify the load-shortening behavior of the cylinder and to influence its buckling load. This influence is especially notable for cylinders in axial compression and for short cylinders under external hydrostatic pressure, where it accounts for a large part of the disagreement between classical theory and experiment.

Further work needed in this field includes studies of cylinders with clamped edges and with flexible rings at the edges. In order to study the behavior of longer cylinders (cylinders of larger Z) in axial compression, it would also be desirable to analyze the semi-infinite cylinder. In addition, in future cylinder studies, it would be useful to extend this work by using a more exact theory for buckling into two circumferential waves for less than three wrinkles in the axial direction.

Langley Research Center,
National Aeronautics and Space Administration,
Langley Station, Hampton, Va., August 20, 1963.

REFERENCES

1. Batdorf, S. B.: A Simplified Method of Elastic-Stability Analysis for Thin Cylindrical Shells. NACA Rep. 874, 1947. (Formerly included in NACA TN's 1341 and 1342.)

2. Batdorf, S. B., Schildcrout, Murry, and Stein, Manuel: Critical Stress of Thin-Walled Cylinders in Axial Compression. NACA Rep. 887, 1947. (Formerly NACA TN 1343.)

3. Donnell, L. H., and Wan, C. C.: Effect of Imperfections on Buckling of Thin Cylinders and Columns Under Axial Compression. Jour. Appl. Mech., vol. 17, no. 1, Mar. 1950, pp. 73-83.

4. Hoff, Nicholas J.: Buckling of Thin Shells. SUDAER No. 114 (AFOSR-TN-61-1422), Dept. Aero. Eng., Stanford Univ., Aug. 1961.

5. Nachbar, W., and Hoff, N. J.: On Edge Buckling of Axially-Compressed, Circular Cylindrical Shells. SUDAER No. 115 (NsG.93-60), Dept. Aero. Eng., Stanford University, Nov. 1961.

6. Stein, Manuel: The Effect on the Buckling of Perfect Cylinders of Prebuckling Deformations and Stresses Induced by Edge Support. Collected Papers on Instability of Shell Structures - 1962. NASA TN D-1510, 1962, pp. 217-225.

7. Föppl, L.: Achsensymmetrisches Ausknicken Zylindrischer Schalen. S.-B. Bayr. Akad. Wiss. 1926, pp. 27-40.

8. Flügge, Wilhelm: Stresses in Shells. Springer-Verlag (Berlin), 1960.

9. Kempner, Joseph: Unified Thin-Shell Theory. Symposium on the Mechanics of Plates and Shells for Industry Research Associates, Polytechnic Inst. of Brooklyn, Mar. 1960.

10. Dow, Marvin B., and Peterson, James P.: Bending and Compression Tests of Pressurized Ring-Stiffened Cylinders. NASA TN D-360, 1960.

11. Fischer, G.: Über den Einfluss der gelenkizen Lagerung auf die Stabilität dünnwandiger Krieszylinder schalen unter Axiallast und Innendruck. Z. Flugwissenschaften, Jahrg. 11, Heft 3, Mar. 1963, pp. 111-119.

12. Stein, Manuel: The Phenomenon of Change in Buckle Pattern in Elastic Structures. NASA TR R-39, 1959.